Cell Reports, Volume *18*

Supplemental Information

Quantitative Map of Proteome Dynamics during Neuronal Differentiation

Christian K. Frese, Marina Mikhaylova, Riccardo Stucchi, Violette Gautier, Qingyang Liu, Shabaz Mohammed, Albert J.R. Heck, A.F. Maarten Altelaar, and Casper C. Hoogenraad

SUPPLEMENTAL TABLES

Table S1 – Related to Figure 1. All proteins quantified in the analysis

Contains the complete proteomics data set containing all identified proteins. ID = unique identifier for each protein; Uniprot = Uniprot accession code; gene name = corresponding gene name; Description = Protein name/description derived from *.fasta database; Σ# Unique Peptides = sum of unique peptides per protein; repl.1 DIV5/DIV1 = log2 fold change between DIV5 and DIV1 from replicate 1; repl.2 DIV5/DIV1 = log2 fold change between DIV5 and DIV1 from replicate 2; repl.1 DIV14/DIV5 = log2 fold change between DIV14 and DIV5 from replicate 1; repl.2 DIV14/DIV5 = log2 fold change between DIV14 and DIV5 from replicate 2; quantified = if a protein was quantified at all time points and in both replicates it is flagged "all"; average log2 DIV5/DIV1 = the average log2 fold-change between DIV5 and DIV1; average log2 DIV14/DIV5 = the average log2 fold-change between DIV14 and DIV5; SAM q-value [%] = q-value derived from statistical analysis of global proteome changes (lower values correspond to higher statistical significance); GProX cluster = cluster derived from fuzzy clustering analysis, related to Figure 2; Protein family = Protein family; Panther protein class = protein class retrieved from pantherdb.org; GO molecular function = Gene ontology molecular function; GO biological process = Gene ontology biological process; GO cellular component = Gene ontology cellular component.

Table S2 – Related to Figure 2. RNA binding proteins

Contains quantitative information about all RNA binding proteins (for column key see description of table S1).

Table S3 – Related to Figure 3. Protein families and complexes

Contains the information on coordinated proteome dynamics of protein families or proteins in complexes. Category = name of protein complex, protein family or gene ontology term; p.value = computed p-value for assessment of significance of co-regulation of the corresponding proteins. P-values were computed using the 'proteinProfile' package within R/bioconductor; ID = unique identified matching to table S1; Uniprot = Uniprot accession code; Gene.name = gene name; Protein.name = corresponding protein name; average log2 DIV5/DIV1 = the average log2 fold-change between DIV5 and DIV1; average log2 DIV14/DIV5 = the average log2 fold-change between DIV14 and DIV5.

Table S4 – Related to Figure 4. Synaptic proteins

Contains quantitative information about synaptic proteins (for column key see description of table S1).

Table S5 – Related to Figure 4. Cell adhesion proteins

Contains quantitative information about cell adhesion proteins (for column key see description of table S1).

Table S6 – Related to Figure 7. Interactors of NCAM1

Contains data from affinity purification mass spectrometry analysis of NCAM1 IPs in adult and young rat brain extracts. Uniprot = Uniprot accession code; gene name = gene name; Description = description of the protein; Σ# PSMs = sum of all peptide-spectrum-matches (PSMs) across all IPs; GFP_control = number of PSM from

GFP-only control IP; NCAM120/140/180 = number of PSM from NCAM120/NCAM140/NCAM180 IPs; p-value NCAM120/140/180 = probability score from SAINT (Significance Analysis of INTeractions, version 2.3.2, http://dx.doi.org/10.1038%2Fnmeth.1541) analysis. $0 \leq p \leq 1$, the higher the score the higher the probability for a given interaction with NCAM1; SAINT probability >0.75 = proteins with a SAINT probability score >0.75 are flagged as 'TRUE'.

SUPPLEMENTAL FIGURES

Figure S1, related to Figure 1, Frese et al.

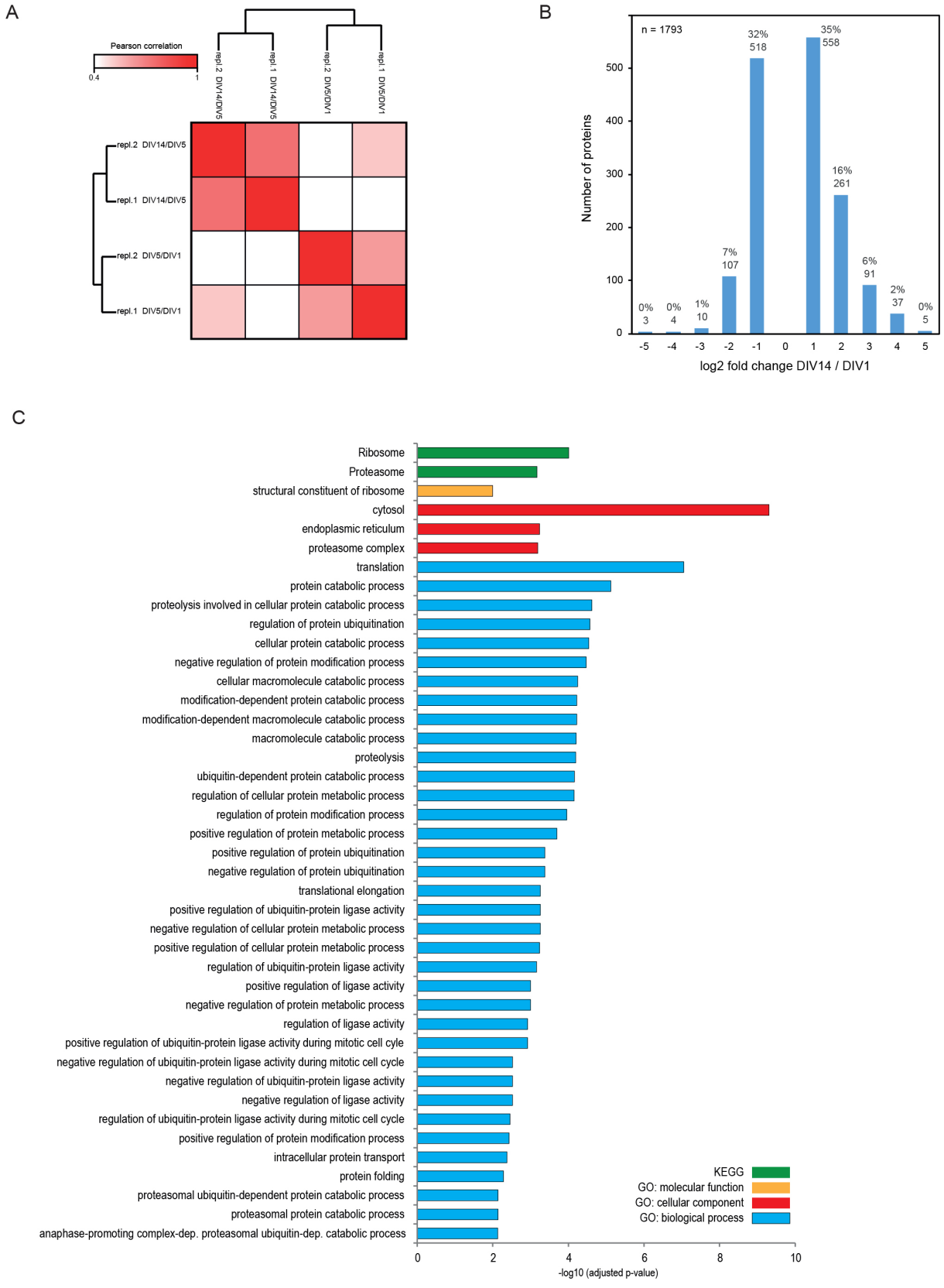

Figure S1 - Related to Figure 1. Reproducibility and statistical analysis of differentially expressed proteins

(A) Heat map showing Pearson correlation scores for the two independent biological replica.

(B) Distribution of fold changes calculated on all the quantified proteins.

(C) Gene ontology (GO) and KEGG pathway enrichment analysis. All quantified proteins were subjected to enrichment analysis with respect to biological process, molecular function, cellular component and protein class (KEGG).

Figure S2, related to Figure 2, Frese et al.

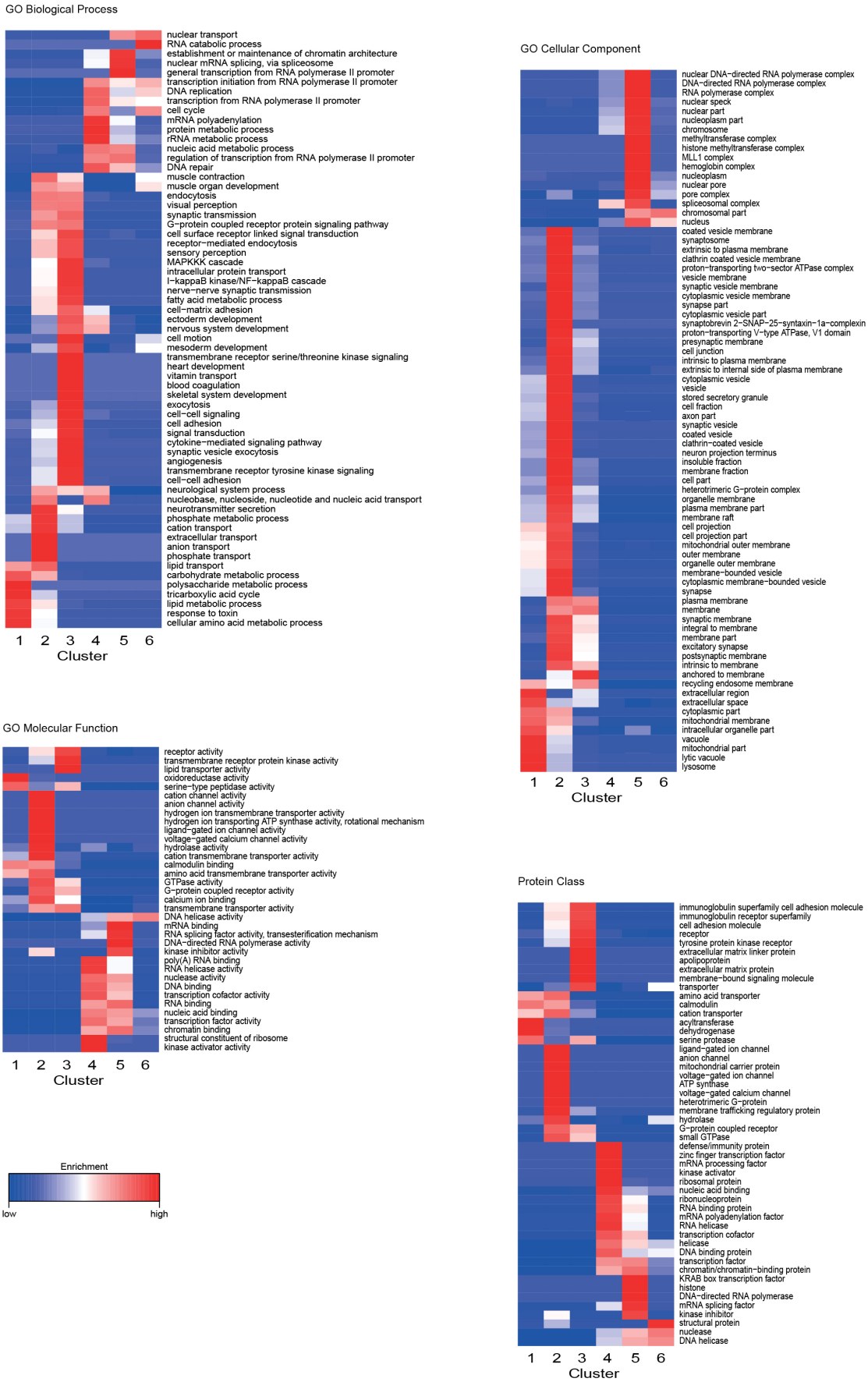

Figure S2 - Related to Figure 2. Gene ontology classification of regulated proteins

For all proteins of each cluster (see Figure 2) enrichment analysis with respect to biological process, molecular function, cellular component and protein class (KEGG) was performed. Overrepresentation was tested against all not regulated proteins. The heat maps show the overrepresentation /underrepresentation of each group in each specific cluster.

Figure S3, related to Figure 3, Frese et al.

A

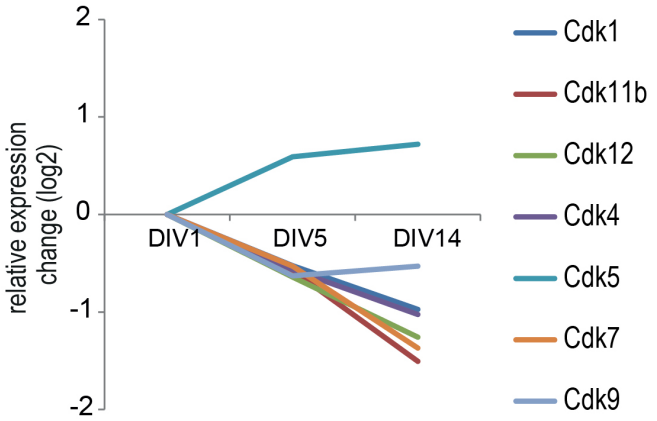

B

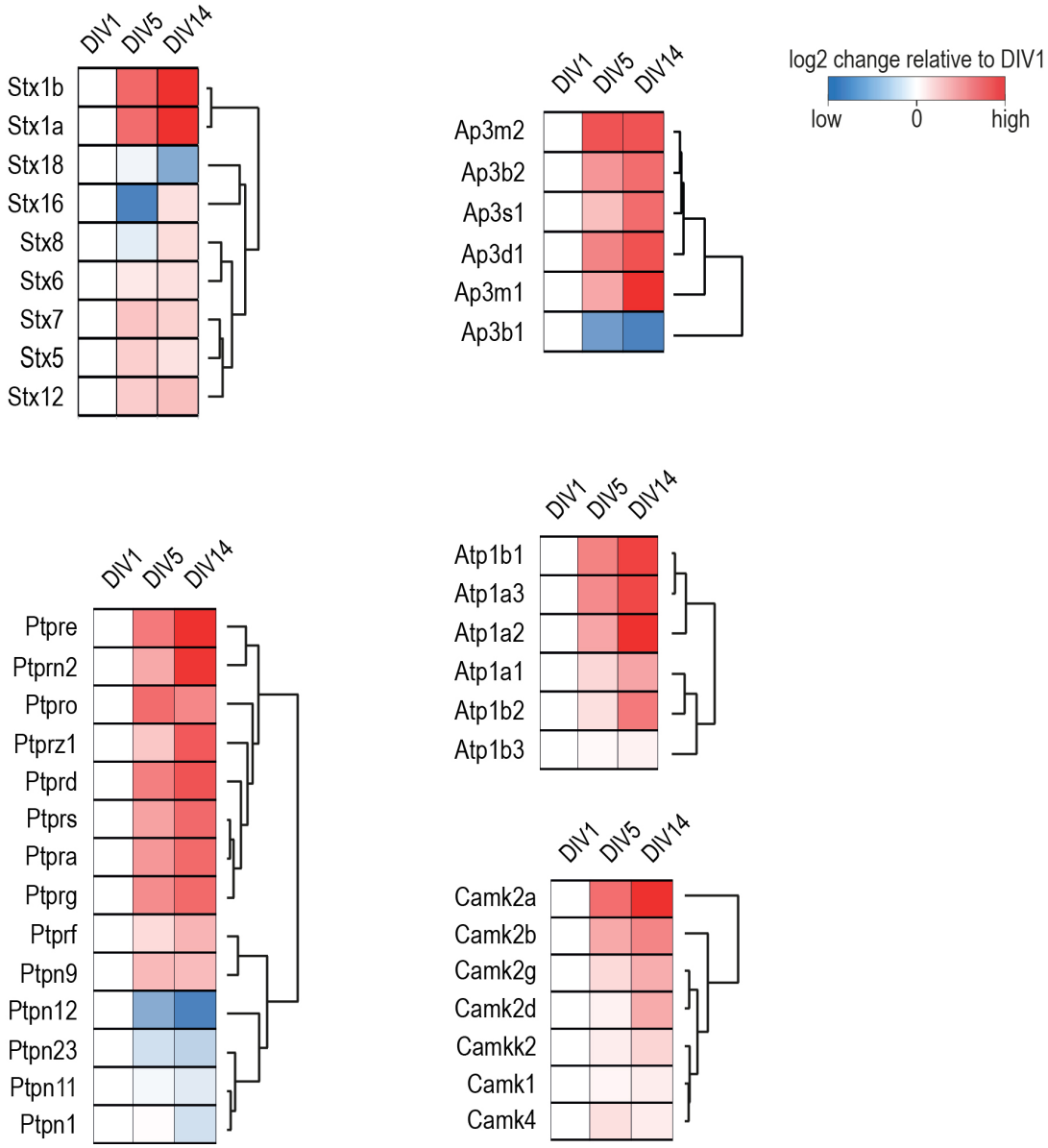

Figure S3 - Related to Figure 3. Expression profiles of protein families/complexes

(A) Expression profiles of proteins from the cyclin-dependent kinase family.

(B) Heat maps of expression profiles of proteins showed in Figure 3B. Ap3b1 (6 unique peptides used for the quantification) does not follow the expression profile of the other AP3 complex proteins. Similar trend has been measured for Atp1b3 (7 unique peptides used for the quantification) that does not change over time while other subunits of the complex are upregulated.

Figure S4, related to Figure 4, Frese et al.

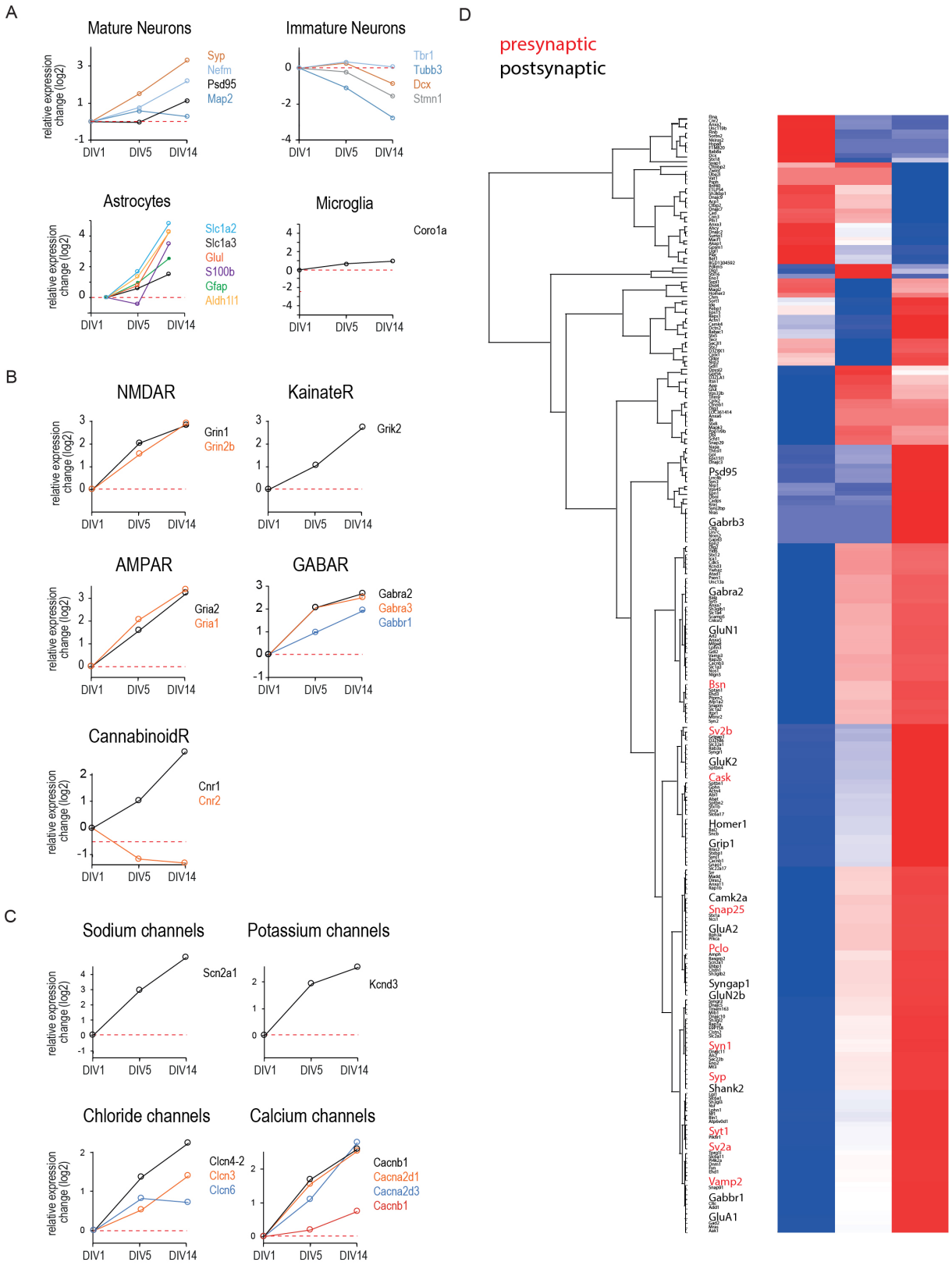

Figure S4 - Related to Figure 4. Expression profiles of cell-type protein markers and proteins with similar function/localization

(A) Expression profiles of selected protein markers for mature neurons, immature neurons, astrocytes and microglia. Astrocytes specific proteins are highly up-regulated after DIV5.

(B) Expression profiles of selected neurotransmitter receptors.

(C) Expression profiles of selected voltage-gated ion channels.

(D) Hierarchical clustering of all synaptic proteins (based on Euclidian distance). Proteins known to be located either pre- or postsynaptic are highlighted in bold. Evidently, the expression profiles of these two subclasses are not distinguishable by hierarchical clustering.

Figure S5, related to Figure 5, Frese et al.

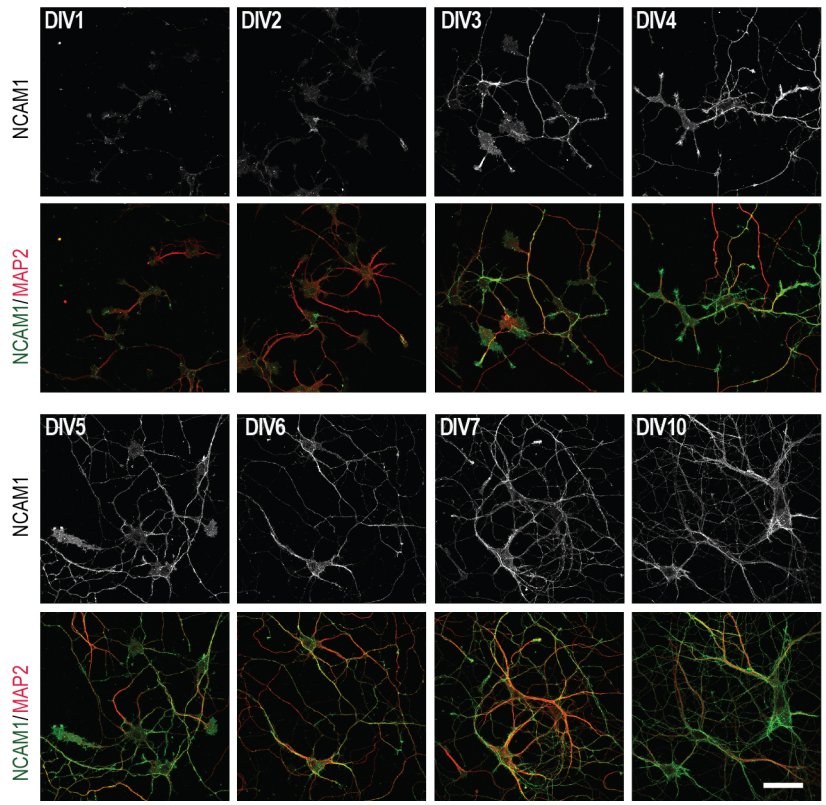

Figure S5 - Related to Figure 5. NCAM1 localization in mouse hippocampal primary neurons

Representative images of mouse hippocampal neurons from DIV1 to DIV10, stained for NCAM1 (green), MAP2 (red). Scale bar, 50 µm.

Figure S6, related to Figure 6, Frese et al.

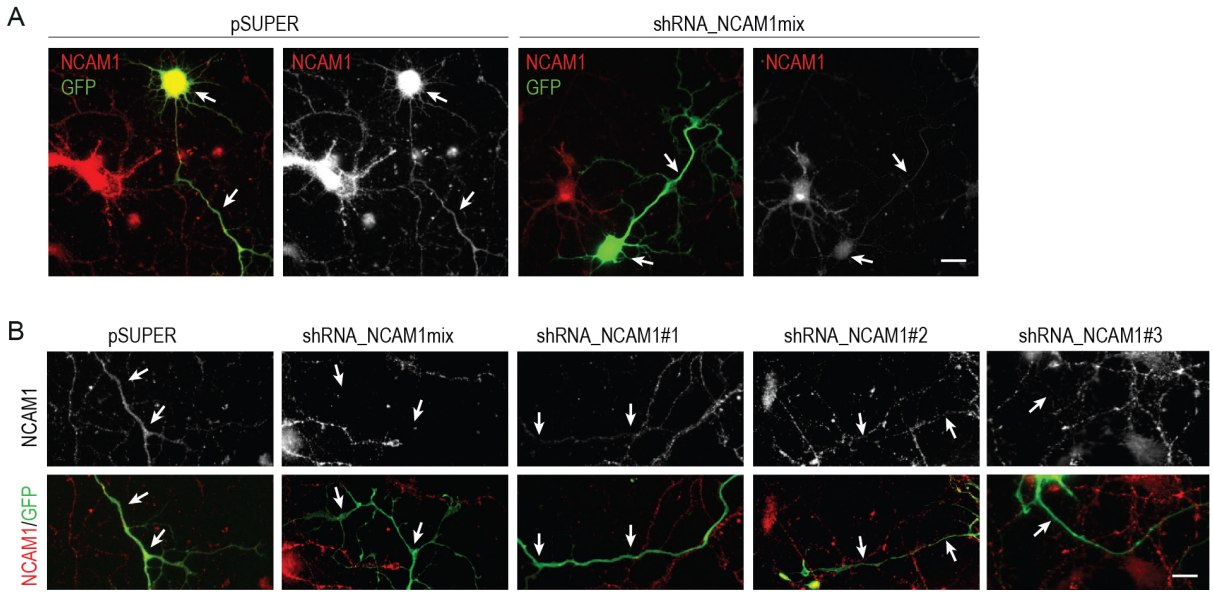

Figure S6 - Related to Figure 6. NCAM1 downregulation in rat hippocampal primary neurons

(A) Representative images of neurons transfected with pSUPER or shRNA NCAM1mix, filled with GFP (1DIV for 3 days) and stained with NCAM1 monoclonal antibody. Scale bar, 20 µm.

(B) Higher magnifications of representative images of neurons co-transfected with pSUPER, shRNA NCAM1mix, shRNA NCAM1#1, shRNA NCAM1#2, shRNA NCAM1#3 and GFP. Arrows point to representative neurites. Scale bar, 10 µm.

Figure S7, related to Figure 7, Frese et al.

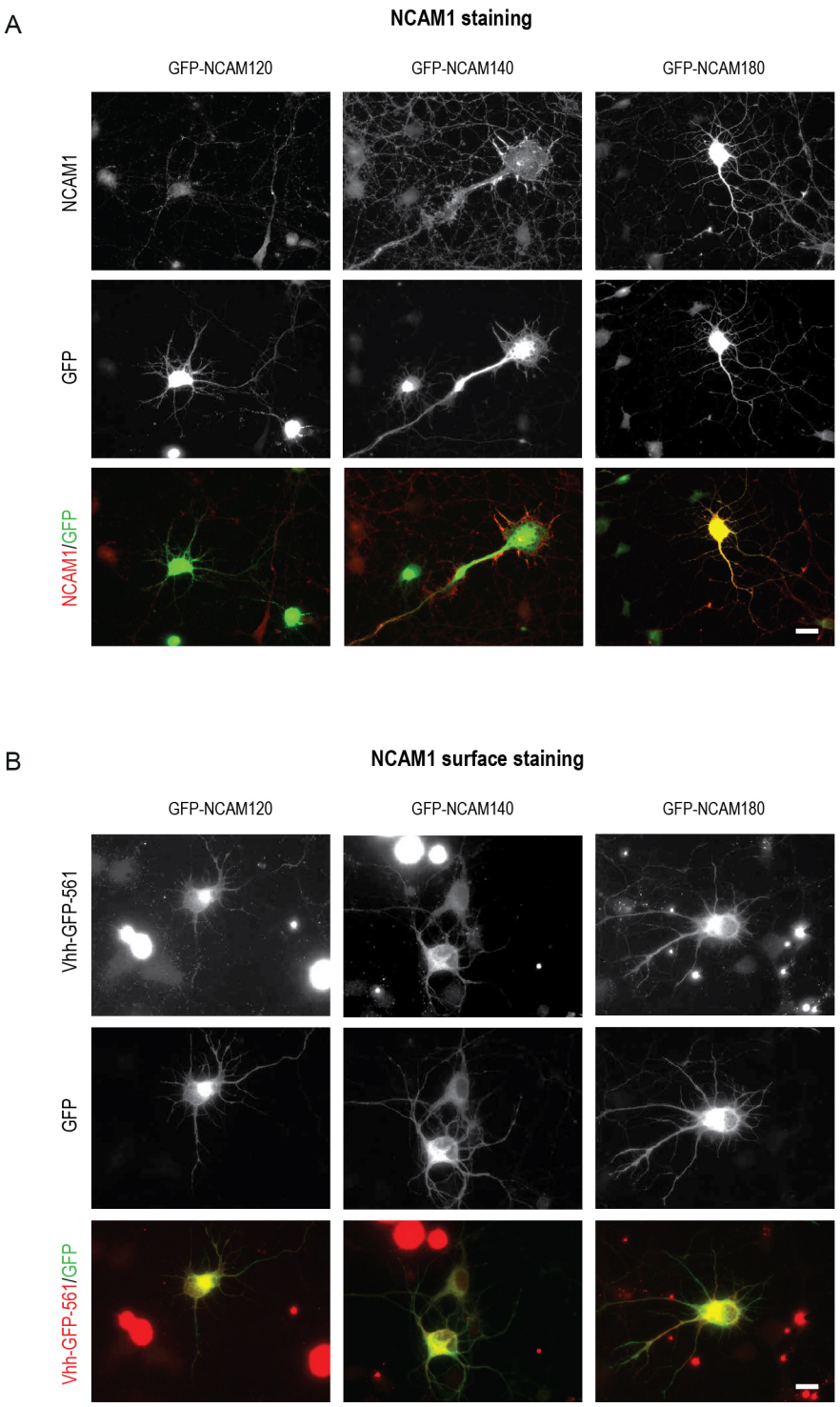

Figure S7 - Related to Figure 7. Characterization of N-terminal GFP tagged NCAM1 isoforms

(A) Representative images of neurons transfected with GFP-NCAM120, GFP-NCAM140 or GFP-NCAM180 and stained with NCAM1 mouse antibody. The NCAM1 antibody recognizes the C-terminal tail of NCAM1 and

as expected the signal is completely overlapping with the GFP only when the longer NCAM1 isoform (NCAM180) is expressed. Scale bar, 20 μm.
(B) Representative images of neurons transfected with GFP-NCAM120, GFP-NCAM140 or GFP-NCAM180 and live stained with Vhh-GFP-568 nanobodies. Cells were not permeabilized before the staining and the GFP-targeted-nanobodies were added directly in the medium at 37°C, so only NCAM1 molecules efficiently expressed on the neuronal surface can be detected. Scale bar, 10 μm.

SUPPLEMENTAL EXPERIMENTAL PROCEDURES

Animals

All experiments with animals were performed in compliance with the guidelines for the welfare of experimental animals issued by the Government of The Netherlands, and were approved by the Animal Ethical Review Committee (DEC) of the Utrecht University.

Antibodies and reagents

The following primary and secondary antibodies were used in this study: NCAM1 mouse (Millipore), NCAM1 rabbit (Proteintech), Syt1, Camk2a mouse (Sigma), PSD95, Cntn1, NCAM2, L1CAM, Kif5B, Actg mouse (Millipore) and Tubα1a rabbit (Abcam), MAP2 rabbit (Cell Signaling), Vhh-GFP-Alexa 561 nanobodies (Yau et al., 2014). Alexa 488-, Alexa 568- and Alexa 594-conjugated secondary antibodies (Invitrogen). Other reagents used in this study include: Jasplakinolide (2792, Tocris Bioscience), n-Dodecyl β-D-maltoside (A0819, Applichem).

Expression vectors and shRNA constructs

The following mammalian expression plasmids have been described: pGW1-GFP (Hoogenraad et al, 2005), pCDNA3.1-RFP-NCAM120, pCDNA3.1-RFP-NCAM140, pCDNA3.1-RFP-NCAM180, pCDNA3.1-eGFP-NCAM120, pCDNA3.1-eGFP-NCAM140, pCDNA3.1-eGFP-NCAM180 (Hata et al., 2007). The following shRNA sequences are used in this study. NCAM1#1 (5'-GGATCTCATCTGGACTTTG), NCAM1#2 (5'-GATCTTCCAGAAGCTCATG) and NCAM1#3 (CGTTGGAGAGTCCAAATTC) targeting rat NCAM1 mRNA (NM_031521.1) were designed using the siRNA selection program at the Whitehead Institute for Biomedical Research (jura.wi.mit.edu/bioc/siRNAext) (Yuan et al., 2004). The complementary oligonucleotides were annealed and inserted into a pSuper vector (Hoogenraad et al., 2005). The control pSuper vector contained a scrambled sequence.

Primary hippocampal neuron cultures and transfection

Rat primary hippocampal cultures were prepared from embryonic day 18 rat brains. Cells were plated on coverslips coated with poly-L-lysine (30μg /ml) and laminin (2μg/ml) at a density of 100,000/well as previously (Kapitein et al., 2010). Hippocampal cultures were grown in Neurobasal medium (NB) supplemented with B27, 0.5 μM glutamine, 12.5 μM glutamate and penicillin/streptomycin. Mouse primary hippocampal cultures were

prepared from embryonic day 18 mouse brains then plated and cultured in the same conditions as rat primary neurons.

Hippocampal neurons were transfected at DIV1 using Lipofectamine 2000 (Invitrogen). Briefly, DNA (1.8 µg/well, for a 12 wells plate) was mixed with 3.3 µl of Lipofectamine 2000 in 200µl NB, incubated for 30 min, and then added to the neurons in NB at 37°C in 5% CO2 for 45 min. Next, neurons were washed with NB and transferred in their original medium at 37°C in 5% CO2 for 3-7 days. For forced actin-stabilization experiments, young neurons co-transfected at day1 were treated 24 hours later (DIV2) with 10 nM Jasplakinolide and cells were then incubated for 6 days at 37°C in the presence of the drug (Swiech et al., 2011).

Primary cortical neuron nucleofection

Primary cortical neurons were isolated from E18 rat brain. Cells (1x106) were transfected using the Amaxa Rat Neuron Nucleofector kit (Lonza) with 3µg of plasmid DNA (pSUPER, ShRNA-NCAM1mix, ShRNA-NCAM1#1, ShRNA-NCAM1#2, ShRNA-NCAM1#3) and plated on coverslips coated with poly-L-lysine (37.5µg/ml) and laminin (5µg/ml) in 12-wells plates (2-6 x104 cells/well) containing DMEM supplemented with 10% FBS (Kaech and Banker, 2006). Cells were allowed to recover and adhere to the surface at 37°C in 5% CO2, after 4 hours the medium was replaced with Neurobasal medium supplemented with 2% B27, 0.5mM glutamine, 15.6µM glutamate, and 1% penicillin/streptomycin. After 4 days cells were lysed in hot denaturing sample buffer.

Sample preparation for Mass spectrometry

At three time points (DIV1, DIV5, DIV14) neurons were washed 4x with 500 µL pre-warmed PBS. For lysis 500 µL lysis buffer (8 M Urea, 1 tablet Complete Mini EDTA-free protease inhibitor Cocktail (Roche) in 10 mL 50 mM triethylammonium bicarbonate (Sigma)) was added to each well. Following sonication, samples were cleared by centrifugation at 20,000 × g for 20 min. Proteins were reduced (5 mM DTT, 55˚C, 30 min), alkylated (10 mM Iodoacetamide, 30 min in the dark) and sequentially digested by LysC (Protein-enzyme ratio 1:50, 37˚C, 4 h) and trypsin (Protein-enzyme ratio 1:50, 37˚C, 16 h) according to the standard filter-aided sample preparation protocol (Wiśniewski et al., 2009). Resulting peptides from each time point were desalted using C18 solid phase extraction cartridges (Waters) and subjected to stable isotope triplex dimethyl labeling on column (Boersema et al., 2009). Labels were swapped between biological replicates. Differentially labeled peptides were mixed in a 1:1:1 ratio based on LC-MS base peak intensity of the separate channels, dried in a vacuum concentrator and reconstituted in 10% formic acid for subsequent fractionation.

Peptide Fractionation

Peptides were fractionated using strong cation exchange chromatography (SCX), as previously described (Frese et al., 2012). Briefly, peptides were loaded onto a Zorbax BioSCX-Series II column (0.8 mm × 50 mm, 3.5 µm) in 100% solvent A (0.05% formic acid in 20% acetonitrile). Solvent B consisted of 0.05% formic acid and 0.5 M NaCl in 20% acetonitrile. Fractionation was conducted using the following gradient: 0−0.01 min (0−2% B); 0.01−8.01 min (2−3% B); 8.01−14.01 min (3−8% B); 14.01−28 min (8−20% B); 28−38 min (20−40% B); 38−48 min (40−90% B); 48−54 min (90% B); 54−60 min (0% B). Collected fractions were dried in vacuo, reconstituted in 10% formic acid/5% DMSO and stored at -80°C prior MS analysis.

Affinity Purification-Mass Spectrometry (AP-MS) using GFP pull-down

Human Embryonic Kidney 293 cells (HEK293) cells were cultured in DMEM/Ham's F10 (50%/50%) containing 10% Fetal Calf Serum (FCS) and 1% penicillin/streptomycin at 37°C and 5% CO2. HEK293 cells were transfected with pGW1-GFP, eGFP-NCAM120, eGFP-NCAM140 and eGFP-NCAM180 constructs with polyethylenimine (PEI, Polysciences) according to the manufacturer instructions. Cells were lysed 48 hours later in a lysis buffer for transmembrane proteins (20mM TrisHCl, 100mM NaCl, 10mM EDTA (pH8.0), 10mM Na4P2O7, 10% Glycerol, 50mM NaF, 1% n-Dodecyl β-D-maltoside, and protease inhibitors (Roche)), centrifuged at 13000 rpm for 15 min and the supernatants were incubated with GFP-trap beads (Chromotek) for 1 hour at 4°C. Beads were then separated using a magnet (Dynal; Invitrogen) and washed five times in washing buffer (20mM Tris HCl, 150mM KCl, 0.1% TritonX-100). Brains were obtained from female adult rats or P5 rat pups and homogenized in 10x volume/weight in tissue lysis buffer (50mM TrisHCl, 150mM NaCl, 0.1% SDS, 0.2% NP-40, and protease inhibitors (Roche)). Brain lysates were centrifuged at 16,000 g for 15 min at 4°C and the supernatant was incubated with the Dynabeads containing GFP or GFP-NCAM120/140/180 for 2 hrs at 4°C and washed with lysis buffer for five times. For MS analysis, the beads were resuspended in 15 ul of 4x Laemmli Sample buffer (Biorad) and supernatants were loaded on a 12% Criterion XT Bis-Tris precast gel (Biorad). The gel was stained with 0.1% Coomassie Brilliant Blue G250 (Sigma-Aldrich, Steinheim, Germany) in 25% methanol and 10% acetic acid (Merck, Darmstadt, Germany). Each lane from the gel was cut in 3 slices, destained and digested using trypsin, as described in (Ekkebus et al., 2013). Briefly, each lane from the gel was cut into three pieces and placed in 0.5-ml tubes. They were washed with 250 µl of water, followed by 15-min dehydration in acetonitrile. Proteins were reduced (10 mM dithiothreitol, 1h at 56°C), dehydrated and alkylated (55 mM iodoacetamide, 1h in the dark). After two rounds of dehydration, trypsin was added to the samples (20 µl of 0.1 mg/ml trypsin in 50 mM Ammoniumbicarbonate) and incubated overnight at 37°C. Peptides were extracted with ACN, dried down and reconstituted in 10% formic acid prior MS analysis.

Mass spectrometry analysis

All samples were analyzed on an ETD enabled LTQ-Orbitrap Elite or Q-Exactive mass spectrometer (Thermo Fisher Scientific, Bremen, Germany) that was coupled to Proxeon EASY-nLC 1000 (Thermo Fisher Scientific, Odense, Denmark). Peptides were loaded onto a trap column (Reprosil C18, 3 µm, 2 cm × 100 µm; Dr. Maisch) with solvent A (0.1% formic acid in water) at a maximum pressure of 800 bar and chromatographically separated over the analytical column (Zorbax SB-C18, 1.8 µm, 50 cm × 75 µm; Agilent) using a 60 min, 90 min or 150 min linear gradient from 7-30% solvent B (0.1% formic acid in acetonitrile) at a flow rate of 150 nL/min. The mass spectrometer was operated in the data-dependent acquisition mode. After a survey scan from 350-1500 m/z the 10 or 20 most abundant peptides were subjected to either HCD or decision tree-guided CID/ETD fragmentation (ddDT) (Frese et al., 2011), respectively. Product ions were detected in the Orbitrap (HCD methods; Resolution 7,500) and linear ion trap (ddDT methods), respectively. Normalized collision energy was set to 35% and 32% for CID and HCD, respectively. Charge state dependent ETD reaction time and supplemental activation were enabled. Charge state screening was enabled and ions with charge states <2+ were excluded from analysis. Samples from in-gel digestion were analyzed using a 90 min gradient.

Mass spectrometry data analysis

All mass spectrometric raw data were processed with Proteome Discoverer (version 1.3, Thermo Scientific, Bremen, Germany), as described in (Frese et al., 2012). Peak lists were generated using a standard workflow. The non-fragment filter was used to simplify ETD spectra. HCD spectra were deisotoped and charge deconvoluted. The TopN filter node was used to filter CID and ETD spectra and to retain the 10 most abundant peaks per 100 Da window. Peptide identification was performed by searching individual peak lists of HCD, ETD-IT and CID-IT against the Uniprot rat database (version 2013_01) concatenated with a list of common contaminants using Mascot (version 2.3, Matrix Science, UK). Trypsin was set as cleavage specificity, allowing a maximum of 2 missed cleavages. Precursor ion mass tolerance was set to 15 ppm. Product ion mass tolerance was set to 0.02 Da (Orbitrap detection) and 0.5 Da (ion trap detection), respectively. Carbamidomethylation (C) was used as fixed modification. Oxidation (M) and dimethylation (light, intermediate or heavy) of lysine residues and the peptide N-termini, respectively, were set as variable modification. The percolator algorithm was used to filter the data to <1% false-discovery-rate on peptide level. Additionally, only peptides that pass the following filters were retained: mascot ion score ≥20, minimum peptide length 6, precursor mass tolerance 10 ppm, and search engine rank 1. Only unique peptides were used for quantification and the obtained ratios were normalized to the median. AP-MS data was analyzed using Proteome Discoverer and the aforementioned settings. Common contaminant proteins including immunoglobulins were removed from the list.

Bioinformatic analysis

Gene ontology (GO) classification was obtained via PANTHER (Mi et al., 2005) and Perseus (version 1.3.0.4, within MaxQuant) (Cox et al., 2009). Enrichment analysis in terms of relative proteins abundance was performed using a Fisher's exact test in Perseus (GO cellular component, min. enrichment factor 3.5, Benjamini-Hochberg corrected p-value <0.02). KEGG pathway analysis and tissue enrichment testing were performed using DAVID (Cox et al., 2009) (Huang da et al., 2009). Hierarchical clustering was performed within Perseus using Euclidian distance. Network analysis was performed using the GeneMania plugin (Montojo et al., 2010) within Cytoscape (Shannon et al., 2003). Significance analysis of microarrays (SAM) (Roxas and Li, 2008) was used to assess significance of obtained protein ratios, as described in (Munoz et al., 2011). Briefly, log2-transformed ratios of proteins that were quantified in all time points and in both replicates were subjected to a one-class test using 1000 permutations and an S0 value based on the method by (Tusher et al., 2001). Proteins with a SAM q-value ≤0.15 (corresponding to a median log2 fold-change of >1.5 between DIV14 and DIV1) were considered significantly regulated and subjected to unsupervised fuzzy clustering using GProX 1.1.9 (Rigbolt et al., 2011). Briefly, the relative abundance of all proteins from each time point was log10 transformed, Z-scored and clustered using a fuzzification value of 2, 100 iterations and a minimum membership value of 0.35. Gene ontology enrichment for each cluster was performed using a Fisher's exact test within GProX (min. occurrences 5 for GOMF, GOBP and protein class, and 1 for GOCC; Benjamini-Hochberg corrected p-value <0.05). Significance of expression profile similarities within groups of interest was determined using the R package "proteinProfiles" (Julian Gehring [2011], https://bioconductor.org/packages/devel/bioc/html/proteinProfiles.html) within R/Bioconductor (Gentleman et al., 2004), as reported elsewhere (Hansson et al., 2012). The heatmap in Figure 7 was generated by subjecting log10-transformed and z-scored relative abundances of all proteins from each time point (DIV 1, 5, 14) to

hierarchical clustering using Euclidean distance. Statistical assessment of the AP-MS data was performed based on spectral counts using the SAINT (Significance Analysis of INTeractions, version 2.3.2) algorithm (Choi et al., 2011). The SAINT parameters were set as follows: nburn=4000, niter=20000, lowmode=0, minfold=1, and norm=1. Bait proteins with a SAINT probability score >0.75 were considered putative protein interaction partners.

Cell extracts and Western blotting

HEK293 cell extracts were prepared by resuspending cells in equal amounts of lysis buffer containing 25mM Tris-HCl pH 8.0, 50mM NaCl, 0.5% Triton X-100 supplemented with 1x protease inhibitors cocktail (Roche). The soluble fraction was separated by centrifugation at 13000 rpm for 15 minutes and supplemented with sample buffer 4x (8% SDS, 25% glycerol, 0.05M Tris pH 6.8, 400mM DTT and 40mg/l bromophenol blue). Rat primary hippocampal neurons (E18) were plated on 24 mm coverslips in 6 well plates and harvested at DIV 1, 5 and 14 days in vitro (DIV), or at DIV2, 4, 6, 8, 10, 12, 14, 16, 18 and 21. Cells were lysed in hot denaturing sample buffer. Lysates prepared from individual wells were pooled together (3 wells each stage, 3 independent preparations) and equal protein concentrations were adjusted before supplementing with 4x sample buffer. Samples were boiled at 99ºC for 10 minutes before being analyzed by SDS PAGE. Proteins were transferred on PVDF membranes (Millipore) using a semi-dry blotting system. Membranes were blocked and incubated with primary antibodies (overnight at 4°C) in PBS or PBST (0.1% Tween-20, 2% BSA). Peroxidase-coupled secondary antibodies were applied for 1 hour at RT. Following primary NCAM1 antibodies have been used for detection: NCAM1 mouse antibody (Millipore 1:1000), NCAM1 rabbit antibody (Proteintech 1:1000). For quantifying NCAM1 expression levels, the relative intensities of NCAM1 for each sample (n=3) were obtained by normalization to the tubulin loading control. The relative percentage of NCAM1 expression levels was obtained by normalization of the relative intensities with the relative intensity of NCAM1 at DIV2. For quantifying Syt1, Camk2a, PSD95, Cntn1, NCAM1, NCAM2, L1CAM expression levels, the relative intensities of each band (n=3) were measured together with 3 different loading controls such as Kif5B, Actg and Tubα1a . Quantifications were performed with Image J.

Immunohistochemistry

For general immunohistochemistry, neurons were fixed for 10 min with 4% paraformaldehyde (PFA)/4% sucrose in phosphate buffered saline (PBS) at room temperature. After fixation cells were washed 3 times for 10 min in PBS at room temperature, incubated for 10 min with permeabilization buffer (0.25% TritonX-100 in PBS) and then blocked for 1 hour with blocking buffer (2% BSA, 2% Glycin, 0.2% Gelatin, 50mM NH4Cl, in PBS). Neurons were then incubated with primary antibodies in blocking buffer overnight at 4°C, washed three times in PBS for 10 min at room temperature and then incubated with the Alexa-conjugated secondary antibodies in blocking buffer for 1 hour at room temperature. Neurons were then washed 3 times for 5 min in PBS at room temperature and subsequently mounted on slides in Vectashield mounting medium (Vector Laboratories). For labeling of F-actin neurons were incubated with Phalloidin-647 (1:100 in PBS; Molecular Probes) for 30 min at room temperature, washed 3 times in PBS and mounted on slides in Mowiol. Images were acquired using a Nikon upright or Olympus BX53 upright fluorescent microscopes with a 10x, 20x or 40x objective. Confocal images were acquired using a Leica SP5 microscope (Wetzlar, Germany) equipped with a

Krypton-Argon-Ion laser (488/568/647 nm) and an acousto-optic-tunable filter (AOTF) for selection and intensity adaptation of laser lines. Images and were taken with 63x oil objective as z-stacks (300 nm z-step) and maximum intensity projections were calculated from each fluorescence channel of the image-stack.

Analyzing NCAM1 knockdown efficiency by immunostaining

Efficiency of NCAM1 shRNA knock down was verified by immunostaining of endogenous NCAM1 protein in hippocampal neurons co-transfected at DIV1 with 0.45 µg/well GFP and 1,35 µg/well of different NCAM1-shRNAs or a mixture of all of them, and fixed 3 days later. NCAM1 staining was measured in neurites of GFP positive neurons and was compared to NCAM1 staining in neurites of GFP negative surrounding cells. Quantifications were performed with Image J software (http://rsb.info.nih.gov/ij).

Quantification of fluorescent intensity. For the quantification of antibody staining, images were acquired with a 40x oil objective with the same settings and the exposure time and ImageJ was used to manually draw specific regions of interest (ROI) located in primary neurites. From the ROIs the mean intensity was measured. To prevent selection bias during quantification, in NCAM1-KD neurons the neurites segments were selected in one channel (GFP) and blindly quantified in the other channel (NCAM1 intensity). Intensities were measured in at least three neurites per neuron, in segments of approximately the same size, both in GFP positives and GFP negatives neurons within the image. To remove the background signal, the intensity near the selected neurites (same segment size) was measured and subtracted to the neurites measured intensities within the same image. Intensities were averaged over multiple cells, normalized and a statistical analysis was performed with student's t test assuming a two-tailed and unequal variation. For Figure 6C, n = 9+9 neurons for pSUPER, n = 13+13 neurons for shNCAM1 mix, n = 7+7 neurons for shNCAM1#1, #2 and #3. n is derived from two independent experiments.

Morphometric analyses of hippocampal neurons

To analyze axonal and dendritic morphology of NCAM1 knockdown neurons, GFP was used as an unbiased cell-fill in combination with different NCAM1-shRNAs or a mixture of all of them. Hippocampal neurons were co-transfected at DIV1 using the same concentrations of plasmid DNA previously reported, and fixed 7 days later. The morphometric analysis and quantification were performed with ImageJ. The axonal parameters, such as axonal total length and longest neurite length, were measured in images acquired with a dry 10x objective whereas quantification of the dendrites total length, primary dendrites length and branches length was done with images acquired with an 20x dry or 40x oil objective. For axon and dendrite length, all neurites of a single neuron were traced in ImageJ and the number of pixels was then converted to distance in µm. Morphological characteristics and MAP2 staining were used as parameters to distinguish axon and dendrites. Data were averaged over multiple cells and experiments, and a statistical analysis was performed with student's t-test assuming a two-tailed and unequal variation. For Figure 6E (axon morphology); n = 18 neurons for pSUPER, n = 25 neurons for shNCAM1mix, n = 17 neurons for shNCAM1#1, n = 16 neurons for shNCAM1#2, n = 18 neurons for shNCAM1#3. For Figure 6F (dendrites morphology): n = 9 neurons for pSUPER, n = 10 neurons for shNCAM1mix, n = 8 neurons for shNCAM1#1, n = 8 neurons for shNCAM1#2, n = 9 neurons for shNCAM1#3. For Figure 7F (axon morphology): n = 9+9 neurons for pSUPER, n = 9+9 neurons for shNCAM1#1, n = 11+11

neurons for shNCAM1#3. For Figure 7G (dendrites morphology): n = 12+12 neurons for pSUPER, n = 12+12 neurons for shNCAM1#1, n = 13+13 neurons for shNCAM1#3. n is derived from two independent experiments.

SUPPLEMENTAL REFERENCES

Boersema, P.J., Raijmakers, R., Lemeer, S., Mohammed, S., and Heck, A.J.R. (2009). Multiplex peptide stable isotope dimethyl labeling for quantitative proteomics. Nat. Protoc. *4*, 484–494.

Choi, H., Larsen, B., Lin, Z.Y., Breitkreutz, A., Mellacheruvu, D., Fermin, D., Qin, Z.S., Tyers, M., Gingras, A.C., and Nesvizhskii, A.I. (2011). SAINT: probabilistic scoring of affinity purification-mass spectrometry data. Nat. Methods *8*, 70–73.

Cox, J., Matic, I., Hilger, M., Nagaraj, N., Selbach, M., Olsen, J. V, and Mann, M. (2009). A practical guide to the MaxQuant computational platform for SILAC-based quantitative proteomics. Nat. Protoc. *4*, 698–705.

Ekkebus, R., Van Kasteren, S.I., Kulathu, Y., Scholten, A., Berlin, I., Geurink, P.P., De Jong, A., Goerdayal, S., Neefjes, J., Heck, A.J.R., et al. (2013). On terminal alkynes that can react with active-site cysteine nucleophiles in proteases. J. Am. Chem. Soc. *135*, 2867–2870.

Frese, C.K., Altelaar, A.F.M., Hennrich, M.L., Nolting, D., Zeller, M., Griep-Raming, J., Heck, A.J.R., and Mohammed, S. (2011). Improved Peptide Identification by Targeted Fragmentation Using CID, HCD and ETD on an LTQ-Orbitrap Velos. J. Proteome Res. *10*, 2377–2388.

Frese, C.K., Altelaar, A.F.M., Van Den Toorn, H., Nolting, D., Griep-Raming, J., Heck, A.J.R., and Mohammed, S. (2012). Toward full peptide sequence coverage by dual fragmentation combining electron-transfer and higher-energy collision dissociation tandem mass spectrometry. Anal. Chem. *84*, 9668–9673.

Gentleman, R.C., Carey, V.J., Bates, D.M., Bolstad, B., Dettling, M., Dudoit, S., Ellis, B., Gautier, L., Ge, Y., Gentry, J., et al. (2004). Bioconductor: open software development for computational biology and bioinformatics. Genome Biol. *5*, R80.

Hansson, J., Rafiee, M.R., Reiland, S., Polo, J.M., Gehring, J., Okawa, S., Huber, W., Hochedlinger, K., and Krijgsveld, J. (2012). Highly Coordinated Proteome Dynamics during Reprogramming of Somatic Cells to Pluripotency. Cell Rep. *2*, 1579–1592.

Hata, K., Polo-Parada, L., and Landmesser, L.T. (2007). Selective targeting of different neural cell adhesion molecule isoforms during motoneuron myotube synapse formation in culture and the switch from an immature to mature form of synaptic vesicle cycling. J. Neurosci. *27*, 14481–14493.

Hoogenraad, C.C., Milstein, A.D., Ethell, I.M., Henkemeyer, M., and Sheng, M. (2005). GRIP1 controls dendrite morphogenesis by regulating EphB receptor trafficking. Nat. Neurosci. *8*, 906–915.

Huang da, W., Sherman, B.T., and Lempicki, R.A. (2009). Systematic and integrative analysis of large gene lists using DAVID bioinformatics resources. Nat. Protoc. *4*, 44–57.

Kapitein, L.C., Yau, K.W., and Hoogenraad, C.C. (2010). Microtubule Dynamics in Dendritic Spines. Methods Cell Biol *97*, 111-132.

Mi, H., Lazareva-Ulitsky, B., Loo, R., Kejariwal, A., Vandergriff, J., Rabkin, S., Guo, N., Muruganujan, A., Doremieux, O., Campbell, et al. (2005). The PANTHER database of protein families, subfamilies, functions and pathways. Nucleic Acids Res. *33*, D284-288.

Montojo, J., Zuberi, K., Rodriguez, H., Kazi, F., Wright, G., Donaldson, S.L., Morris, Q., and Bader, G.D. (2010). GeneMANIA cytoscape plugin: Fast gene function predictions on the desktop. Bioinformatics *26*, 2927–2928.

Munoz, J., Low, T.Y., Kok, Y.J., Chin, A., Frese, C.K., Ding, V., Choo, A., and Heck, A.J.R. (2011). The quantitative proteomes of human-induced pluripotent stem cells and embryonic stem cells. Mol. Syst. Biol. *7*, 1–13.

Rigbolt, K.T.G., Vanselow, J.T., and Blagoev, B. (2011). GProX, a user-friendly platform for bioinformatics analysis and visualization of quantitative proteomics data. Mol. Cell. Proteomics *10*, O110.007450.

Roxas, B.A., and Li, Q. (2008). Significance analysis of microarray for relative quantitation of LC/MS data in proteomics. BMC Bioinformatics *9*, 187.

Shannon, P., Markiel, A., Ozier, O., Baliga, N.S., Wang, J.T., Ramage, D., Amin, N., Schwikowski, B., and Ideker, T. (2003). Cytoscape: A software Environment for integrated models of biomolecular interaction networks. Genome Res. *13*, 2498–2504.

Swiech, L., Blazejczyk, M., Urbanska, M., Pietruszka, P., Dortland, B.R., Malik, A.R., Wulf, P.S., Hoogenraad, C.C., and Jaworski, J. (2011). CLIP-170 and IQGAP1 cooperatively regulate dendrite morphology. J. Neurosci. *31*, 4555–4568.

Tusher, V.G., Tibshirani, R., and Chu, G. (2001). Significance analysis of microarrays applied to the ionizing radiation response. Proc. Natl. Acad. Sci. USA *98*, 5116–5121.

Wiśniewski, J.R., Zougman, A., Nagaraj, N., and Mann, M. (2009). Universal sample preparation method for proteome analysis. Nat. Methods *6*, 359–362.

Yuan, B., Latek, R., Hossbach, M., Tuschl, T., and Lewitter, F. (2004). siRNA selection server: An automated siRNA oligonucleotide predicition server. Nucleic Acids Res. *32*, W130-134.